CHAPTER 8

PROGRESS IN ENERGY DENSITY

The present chapter highlights the progress in energy density $(BH)_{max}$ of RE-free strontium hexaferrite based magnets, which is a key figure of merit for magnet performance.

8.1 Introduction

Nowadays, the choice of permanent magnets depends on a balanced evolution of worth and performance. It requires the development of high-performance rare-earth free magnets having comparable properties to NdFeB. $(BH)_{max}$ is the key figure of merit for the performance evaluation of permanent magnets. A high value of $(BH)_{max}$ is desirable that can be obtained with high H_c and M_s values. For the practical involvement of the strontium hexaferrite based non-rare-earth magnets, high $(BH)_{max}$ is required for adequate power and torque generation, high H_c is essential for high demagnetization resistance, high M_s is important to gain high M_r leading to higher $(BH)_{max}$ value and helps in product miniaturization, and also high T_c is required to ensure good operating efficiency.

8.2 Calculation of Energy Density

Energy density is estimated by the highest rectangular area that can be best fitted in the demagnetization curve, i.e., II-quadrant of the *B-H* loop. The *B-H* loop is obtained by the following conversion in the magnetic moment (*M*) to get the magnetic induction (*B*):

In the CGS unit, $B = 4\pi M + H$ (8.1)

Conversion of magnetic moment *M* from emu/g to kG,

$$M\,(\text{emu/cm}^3) = M(\text{emu/g}) \times density\ (\text{g/cm}^3) \quad (8.2)$$

$$1\ \text{emu/cm}^3 = 1\ \text{kA/m} = (4\pi)\ \text{kOe} \quad (8.3)$$

$$1\ \text{kOe} = 1\ \text{kG} \quad (8.4)$$

8.3 Energy density and Curie Temperature

From the material's engineering point of view, high $(BH)_{max}$ requires the principal source of exceptional anisotropy (Lewis & Jiménez-Villacorta, 2013), and hence a high H_c value along with a high M_s. Based on the current improvement in magnetic properties, best of three compositions from different series of the thesis work [$SrFe_8Al_4O_{19}$_3wt%Bi_2O_3 from chapter 6, $SrFe_{8.985}Ni_{0.015}Al_3O_{19}$ from chapter 5, and $SrFe_{7.8}Al_4Zn_{0.2}O_{19}$ from chapter 7] is selected here to demonstrate the enhancement in $(BH)_{max}$. These compositions are selected due to their high H_c (either nearly approaching the H_c of NdFeB ~15.07 kOe or even higher than that) and better M_s value. Not only high $(BH)_{max}$ but also a high Curie temperature (T_c) is required to be fulfilled for practical applications. T_c is also analyzed for the proposed compositions to ensure good thermal stability and operating temperature efficiency.

8.3.1 A Composition of $SrFe_8Al_4O_{19}$_3 wt% Bi_2O_3, (1050°C)

The energy density estimation of $SrFe_8Al_4O_{19}$_xBi_2O_3 (x = 3 wt%) hexaferrite sintered at 1050°C is shown in Fig. 8.1. In the magnetic study, M_s of 16.42 emu/g and H_c of 9.78 kOe is obtained for this composition, which results in a $(BH)_{max}$ value of 5.5 MGOe. For this sample, the highest value of both M_r and bH_c is obtained, which results in the maximum energy density. In comparison to the commercial SrM magnet having $(BH)_{max}$ ~4 MGOe, a slight improvement in $(BH)_{max}$ of $SrFe_8Al_4O_{19}$ is observed with the 3 wt% Bi_2O_3 sintering aid doping and 1050°C sintering temperature. It can be used in low-power rated motor applications. Also, it can be used in other permanent magnet applications where the device size is not an issue; then, high $(BH)_{max}$ can be achieved accordingly by increasing the magnet volume.

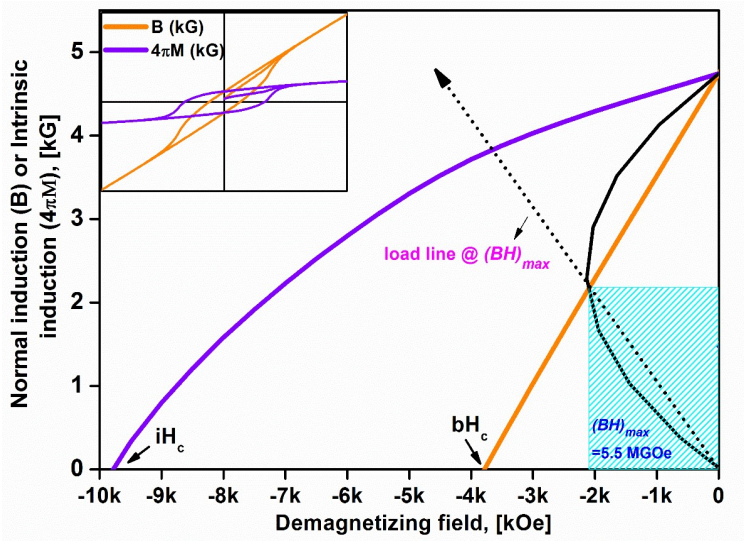

Figure 8.1 *Energy density $(BH)_{max}$ of $SrFe_8Al_4O_{19}$_xBi_2O_3 (x = 3 wt%) hexaferrite sintered at 1050°C, estimated from demagnetization curve, where iH_c is intrinsic coercivity & bH_c is magnetic induction coercivity.*

The *M* vs. *T* analysis of $SrFe_8Al_4O_{19}$_xBi_2O_3 (x = 3 wt%) hexaferrite sintered at 1050°C is shown in Fig. 8.2. It was analyzed under a 300 Oe constant magnetic field to determine the Curie transition. For this composition, magnetic transition indicates the T_c ~724 K. The magnetic moment is observed to decrease with the temperature, so it is expected that the magnetization vector can only lay along two (up and down) directions in the structure (Soria et al., 2019). It is reasonable due to the strong uniaxial character of SrM magnet.

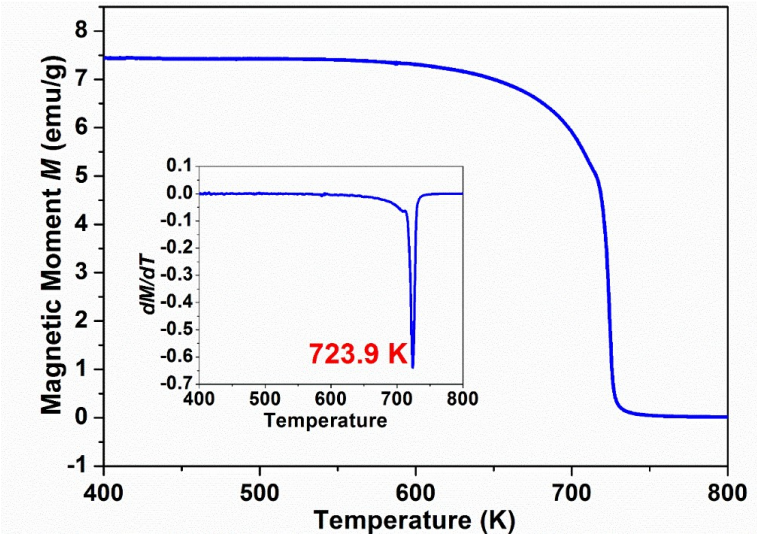

Figure 8.2 *M-T curve of $SrFe_8Al_4O_{19}$_xBi_2O_3 (x = 3 wt%) hexaferrite sintered at 1050°C.*

8.3.2 A Composition of $SrFe_{8.985}Ni_{0.015}Al_3O_{19}$

In the magnetic study, the H_c value of 17.12 kOe is obtained with 20.1 emu/g of M_s for the $SrFe_{8.985}Ni_{0.015}Al_3O_{19}$ composition, which is overall better than the previously reported higher values of hard magnetic parameters (Chen et al., 2008; Liu et al., 2011; Luo et al., 2012; Ma et al., 2016; Shekhawat & Roy, 2019; Torkian et al., 2016; Trusov et al., 2018; Wang et al., 2012, 2017). A 16.2 MGOe value of $(BH)_{max}$ is estimated for this composition and shown in Fig. 8.3. High M_r value due to single magnetic domain formation and high H_c value of the composition is the reason for such a high value of $(BH)_{max}$. It will also increase the magnetic torque of the motor; therefore, the irreversible demagnetization triggered by field weakening flux will not arise early. The high H_c value of the $SrFe_{8.985}Ni_{0.015}Al_3O_{19}$ (17.12 kOe) composition is even higher than the NdFeB (15.07 kOe) magnets, which will also rectify the drawback of demagnetization risk in ferrite based motor applications. The obtained results indicate a strong potential of SrM-based magnet to be utilized in high-power motor applications.

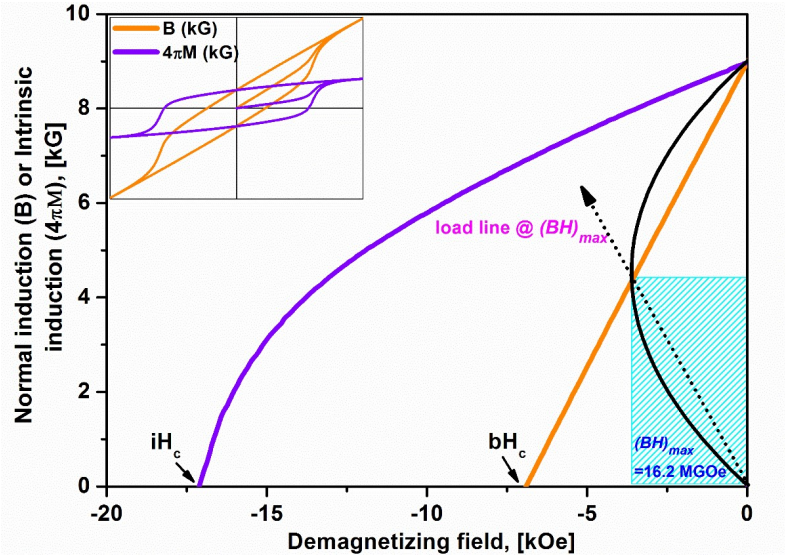

Figure 8.3 *Energy density $(BH)_{max}$ of $SrFe_{8.985}Ni_{0.015}Al_3O_{19}$ hexaferrite, estimated from demagnetization curve, where iH_c is intrinsic coercivity & bH_c is magnetic induction coercivity.*

The *M* vs. *T* analysis of $SrFe_{8.985}Ni_{0.015}Al_3O_{19}$ hexaferrite magnet is shown in Fig. 8.4. It was analyzed under a 300 Oe constant magnetic field to determine the Curie transition. The shape of *M-T* curve demonstrates the characteristic behavior of Hopkinson effect, which is related to the huge reduction in particle size (Buzinaro et al., 2016). The selected synthesis process of sol-gel auto-combustion might be the reason behind this, which resulted in a small size of particles. When the particle size is decreased below a critical value, magnetic anisotropy starts to decrease due to the thermal effect and the magnetic moment in a material starts to show a non-uniform behavior. Therefore, superparamagnetic relaxation occurs, resulting in a sharp peak (T_{pk} ~ 728 K) near the transition temperature (T_c ~ 732 K), which indicates the transition from a ferromagnetic to a superparamagnetic state. The temperature at which a sudden increase in the magnetic moment takes place is defined as the blocking temperature (T_b ~ 724 K); below this temperature entire particles are expected to be in a magnetically stable state. When temperature overcomes this T_b, superparamagnetic relaxation occurs in the material.

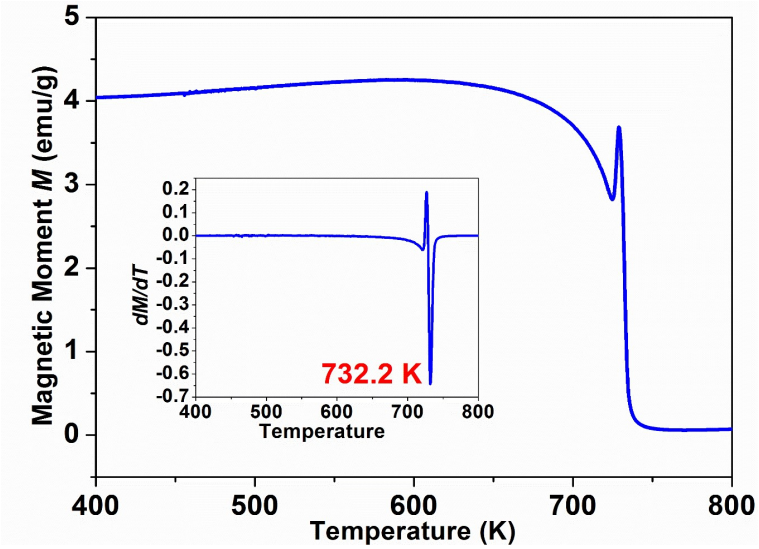

Figure 8.4 *M-T curve of $SrFe_{8.985}Ni_{0.015}Al_3O_{19}$ hexaferrite magnet.*

8.3.3 A Composition of $SrFe_{7.8}Al_4Zn_{0.2}O_{19}$

In the magnetic study, a drastic reduction in M_s of $SrFe_8Al_4O_{19}$ is tried to compensate with Zn^{2+} substitution and succeeded in retaining at least M_s of > 20 emu/g in all Zn-substituted samples. For the $SrFe_{7.8}Al_4Zn_{0.2}O_{19}$ composition, a very large H_c of 18.51 kOe is observed with M_s of 21.87 emu/g. The obtained H_c value is higher than some other reported H_c values in Al-substituted SrM hexaferrite (Luo et al., 2012; Stingaciu et al., 2021; Wang et al., 2012, 2017) and even higher than the H_c of NdFeB magnet (15.07 kOe (Wang et al., 2012)). A large H_c is highly desirable for a high-performance permanent magnet, which provides significant resistance to demagnetization during operation. For the $SrFe_{7.8}Al_4Zn_{0.2}O_{19}$ compositions, a $(BH)_{max}$ of 19.15 MGOe is obtained and shown in Fig. 8.5. It is not equivalent to NdFeB (~ 50 MGOe) but still much better than the $(BH)_{max}$ of commercial SrM magnets (~4 MGOe). It represents a little successful step towards our objective. In motor applications, the performance of these permanent magnets can be further improved with different arrangements of hexaferrite magnets in rotor structure (Kakihara et al., 2013), which will help to make better use of generated field flux by magnets. The modified rare-earth free strontium hexaferrite magnets suggest the possibility of using strontium hexaferrites in high-performance motor drives as per the application requisites.

The M vs. T analysis of $SrFe_{7.8}Al_4Zn_{0.2}O_{19}$ hexaferrite magnet is shown in Fig. 8.6. It was analyzed under a 300 Oe constant magnetic field to determine the Curie transition. Similar characteristic behavior of Hopkinson effect is also observed here in the shape of M-T curve as observed for $SrFe_{8.985}Ni_{0.015}Al_3O_{19}$ (Fig. 8.4). The superparamagnetic relaxation occurs in this composition too, resulting in a sharp peak (T_{pk} ~ 688 K) near the transition temperature (T_c ~ 693 K), which indicates the transition from ferromagnetic to superparamagnetic state. The temperature at which a sudden increase in the magnetic

moment takes place is defined as the blocking temperature (T_b ~ 683 K) below which entire particles are expected to be in a magnetically stable state.

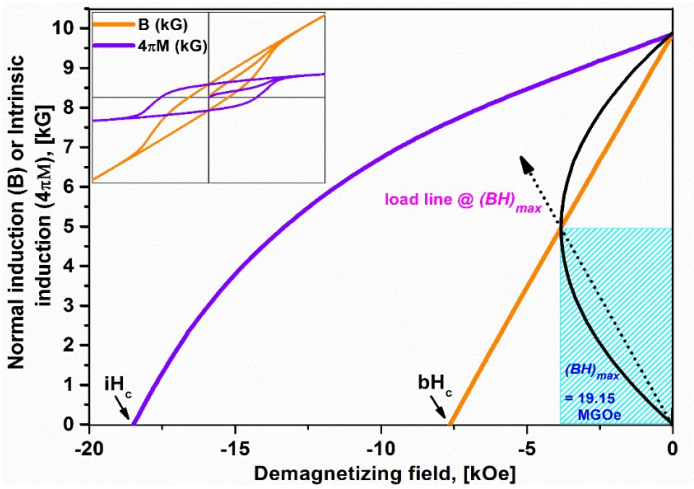

Figure 8.5 *Energy density $(BH)_{max}$ of $SrFe_{7.8}Al_4Zn_{0.2}O_{19}$ hexaferrite, estimated from demagnetization curve, where iH_c is intrinsic coercivity & bH_c is magnetic induction coercivity.*

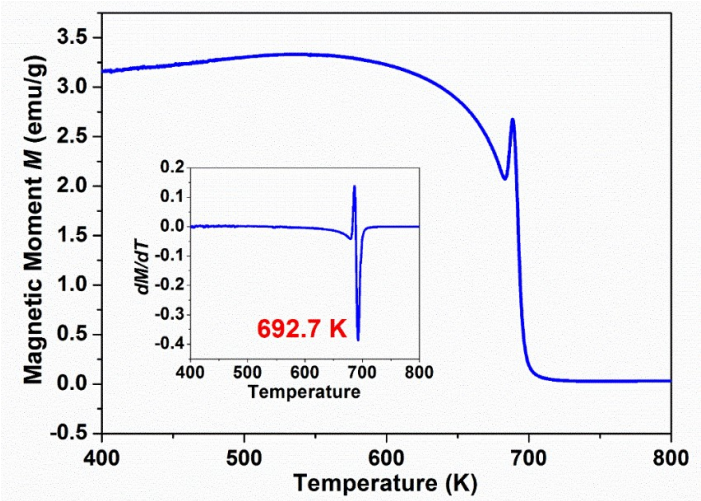

Figure 8.6 *M-T curve of $SrFe_{7.8}Al_4Zn_{0.2}O_{19}$ hexaferrite magnet.*

8.4 Conclusions

For evaluation of the progress in magnetic properties of proposed compositions, essential parameters for permanent magnet are tabulated in Table 8.1 with some commercially available strontium hexaferrite magnet data. It indicates a good improvement in the magnetic properties of modified SrM-based magnets (thesis work). It indicates that

strontium hexaferrites can be used in high-rated permanent magnet applications and can also withstand higher currents without significant performance degradation due to their high Curie temperature, high electrical resistivity, and good thermal stability.

Table 8.1 *A comparative evaluation of progress in energy density and other magnetic properties of modified SrM magnets (thesis work) with some commercially available strontium hexaferrite magnets (*Mahindra CIE, DELTA, TyTek, Alliance*).*

Sr. No.	Company Name (Grade)	Magnetic Properties		
		B_r (T)	H_c (kA/m)	$(BH)_{max}$ (MGOe)
1.	TyTek Industries, Ohio, US (Ceramic 8B)	0.40	244	3.8
2.	Alliance LLC, Indiana, US (C12)	0.45-0.47	274-298	4.8-5.2
3.	Mahindra CIE, India (CS 8B)	0.43-0.45	238-270	4.4-4.8
4.	Delta Manufacturing Ltd., India (DM 7B)	0.41-0.42	332-348	4.1-4.5
a)	$SrFe_8Al_4O_{19}$ _3 wt% Bi_2O_3, (1050 ^{o}C) [thesis work]	0.47	778	5.5
b)	$SrFe_{8.985}Ni_{0.015}Al_3O_{19}$ [thesis work]	0.89	1362	16.2
c)	$SrFe_{7.8}Al_4Zn_{0.2}O_{19}$ [thesis work]	0.98	1473	19.2